Emerging Magnetic Resonance Imaging Techniques for Atherosclerosis Imaging

Wüst, Rob C I; Calcagno, Claudia; Daal, Mariah R R; Nederveen, Aart J; Coolen, Bram F; Strijkers, Gustav J

published in
Arteriosclerosis, Thrombosis, and Vascular Biology
2019

DOI (link to publisher)
10.1161/ATVBAHA.118.311756

document version
Publisher's PDF, also known as Version of record

ATVB in Focus
Atherosclerosis Imaging

Series Editor: Zahi A. Fayad

Emerging Magnetic Resonance Imaging Techniques for Atherosclerosis Imaging

High Magnetic Field, Relaxation Time Mapping, and Fluorine-19 Imaging

Rob C.I. Wüst, Claudia Calcagno, Mariah R.R. Daal, Aart J. Nederveen, Bram F. Coolen, Gustav J. Strijkers

Abstract—Atherosclerosis is a prevalent disease affecting a large portion of the population at one point in their lives. There is an unmet need for noninvasive diagnostics to identify and characterize at-risk plaque phenotypes noninvasively and in vivo, to improve the stratification of patients with cardiovascular disease, and for treatment evaluation. Magnetic resonance imaging is uniquely positioned to address these diagnostic needs. However, currently available magnetic resonance imaging methods for vessel wall imaging lack sufficient discriminative and predictive power to guide the individual patient needs. To address this challenge, physicists are pushing the boundaries of magnetic resonance atherosclerosis imaging to increase image resolution, provide improved quantitative evaluation of plaque constituents, and obtain readouts of disease activity such as inflammation. Here, we review some of these important developments, with specific focus on emerging applications using high-field magnetic resonance imaging, the use of quantitative relaxation parameter mapping for improved plaque characterization, and novel ^{19}F magnetic resonance imaging technology to image plaque inflammation. **(*Arterioscler Thromb Vasc Biol*. 2019;39:841-849. DOI: 10.1161/ATVBAHA.118.311756.)**

Key Words: atherosclerosis ■ fluorine ■ inflammation ■ magnetic resonance imaging

Atherosclerosis is a systemic disease of the intermediate and large arteries that progress for decades before it is diagnosed. Although some may never experience any sign and symptoms of disease, in most people atherosclerosis eventually manifests with acute or chronic symptoms of poor organ perfusion (eg, angina, *claudicatio intermittens*). Acute disease manifestations, such as myocardial infarction and stroke, may be life-threatening.[1] Therefore, early diagnosis and treatment is crucial.

Please see https://www.ahajournals.org/atvb/atvb-focus for all articles published in this series.

Postmortem pathological studies have provided significant insights on the atherosclerotic plaque phenotypes linked to different manifestations of disease.[2] Such studies have spurred high interest in developing and validating diagnostics to identify and characterize at-risk plaques noninvasively and in vivo and improve the stratification of patients with cardiovascular disease.

Magnetic resonance imaging (MRI) of the arterial vessel wall is uniquely positioned to address these diagnostic needs.[3] Since MRI does not deliver any ionizing radiation, it is well suited for repeated, longitudinal examinations to follow-up the progression of atherosclerotic plaque. Its excellent soft tissue contrast and the ability to discriminate not only the vessel lumen but also the vessel wall in high resolution allow measuring plaque size and thickness with accuracy. Furthermore, MRI-based phenotyping of vulnerable plaque components, such as intraplaque hemorrhage, lipid-rich necrotic core, and thin fibrous cap, can be performed based on their appearance in different image weightings (eg, T1, T2, and proton density [PD]). These kind of techniques have been demonstrated to improve risk assessment of subsequent cardiovascular events[4–9] and to be useful as surrogate imaging markers of drug efficacy.[10–15]

However, several challenges still need to be addressed before these key features of vessel wall MRI can be fully leveraged to diagnose and characterize atherosclerotic disease in clinical settings.

First, vessel wall MRI requires imaging with high spatial resolution to accurately quantify atherosclerotic plaque size and thickness and identify plaque components even in relatively small arteries, such as the ones of the intracranial or

Received on: November 29, 2018; final version accepted on: March 12, 2019.

From the Biomedical Engineering and Physics (R.C.I.W., M.R.R.D., B.F.C., G.J.S.) and Radiology and Nuclear Medicine (A.J.N.), Amsterdam Cardiovascular Sciences, Amsterdam UMC, University of Amsterdam, the Netherlands; and Department of Radiology, Translational and Molecular Imaging Institute, Icahn School of Medicine at Mount Sinai, New York (C.C., G.J.S.).

Correspondence to Gustav J. Strijkers, PhD, Amsterdam UMC, University of Amsterdam, Meibergdreef 9, Amsterdam 5600MB, the Netherlands. Email g.j.strijkers@amc.uva.nl

Nonstandard Abbreviations and Acronyms	
CSF	cerebrospinal fluid
3D	3-dimensional
MR	magnetic resonance
MRI	magnetic resonance imaging
PD	proton density
SNR	signal-to-noise ratio

coronary circulation. Ideally, imaging should be performed using 3-dimensional (3D) techniques, with extended coverage along a vascular territory for a comprehensive assessment of disease.[16,17] Imaging voxels should have submillimetric 3D isotropic resolution to better visualize and quantify disease in tortuous vessels, while minimizing partial volume artifacts. Unfortunately, because of intrinsic magnetic resonance (MR) signal limitations, high-resolution 3D acquisitions are very lengthy at the most commonly used field strengths of 1.5 T and 3 T, not well tolerated by patients, prone to pulsatility or bulk motion artifacts, and affected by relatively poor signal-to-noise. Up to now, spatial resolutions of 0.6 to 0.7 mm (isotropic) have been achieved with a good signal-to-noise and acquisition times tolerable for patients.[16,17] However, this may not be sufficient to quantify disease burden and characterize plaque phenotype in the intracranial and coronary arteries.

Furthermore, the quantification of different plaque components related to vulnerability (Figure 1A) currently relies on their identification and segmentation on T1-, T2-, and PD-weighted images.[4,18] Although certainly valuable in patients with established disease, this approach does not allow for the screening and assessment of the progression of atherosclerosis in patients with less advanced lesions. Alternatively, plaque phenotype can be better characterized with the use of MR contrast agents, such as gadolinium-based agents or iron oxides to quantify, respectively, plaque permeability or the presence of inflammatory cells (see also Quantifying Contrast Agent Dynamics).[19] However, safety concerns regarding their long-term tissue accumulation may limit the use of these agents in future clinical practice.[20,21] Furthermore, since their plaque accumulation can only be measured indirectly by quantifying resulting changes in tissue T1 and T2(*), these approaches may be affected by limited sensitivity and specificity.

Several technological strategies are currently being explored to surpass these challenges and improve the characterization of atherosclerosis by MRI. Among these numerous efforts, in this review, we will specifically focus on recent developments aimed at (1) improving the quantification of plaque burden by achieving higher spatial resolution and signal-to-noise at 7 T (ultra-)high field, (2) advancing the characterization of early or less advanced plaques using quantitative T1 and T2(*) mapping, and (3) directly quantifying plaque inflammation using fluorine (^{19}F) MRI.

High Magnetic Field

Vascular MRI may significantly benefit from the use of high magnetic field strength scanners (7 T and higher). The increased signal-to-noise ratio (SNR) associated with higher field MRI can be used to increase spatial resolution, needed to accurately quantify plaque size and to identify relevant vulnerable plaque components. However, to fully benefit from the intrinsically higher SNR, there are several challenges associated with high magnetic fields that need to be overcome. Since clinical 7 T scanners currently lack a body coil, local transmit coils are required. This may result in inhomogeneous B1 transmit fields, particularly when coil geometry is complicated by anatomic constraints such as the carotid arteries in the neck. Furthermore, optimal fat suppression, efficient blood saturation, and—for the brain—cerebrospinal fluid (CSF) suppression are essential to appreciate the vessel wall and (intra-) plaque components which can also be negatively affected by B1 inhomogeneities.

Carotid Arteries

Thus far, there have been only a handful of studies demonstrating feasibility of human carotid artery vessel wall imaging at 7 T. The neck anatomy requires a custom radiofrequency coil design with transmit and receive capabilities. After some preliminary conference reports on prototype 7 T carotid artery coils,[22–24] a first journal article on a 7 T transmit/receive radiofrequency array for imaging of the carotid arteries was published by Kraff et al[25] in 2011. Their design consisted of a 2×4-channel transmit/receive array to cover both sides of the neck. The in vivo imaging protocol was applied to a healthy person and a patient with a known ulcerating plaque with 50% stenosis and consisted of 3D-FLASH (fast low angle shot) bright-blood imaging as well as a PD/T2-weighted turbo-spin-echo sequence to depict the vessel wall and plaque. The images confirmed the extent of stenosis in the patient and revealed the ulcerating plaque. This study demonstrated that (ultra-)high field in vivo MRI of carotid artery plaque is feasible and has clinical potential to reveal plaque components. However, there are still considerable technical challenges associated with 7 T, including specific absorption rate restrictions, inhomogeneous transmit fields, and high field–related artifacts.

Kröner et al[26] provided a first direct comparison of 3 T and 7 T carotid imaging to evaluate whether the advantages of the expected gain in SNR and image resolution at 7 T outweigh the increased technical difficulties associated with imaging at high field. Both carotid arteries of healthy volunteers were imaged with a 2× single-loop transmit/receive coil for 7 T and a 2× single-loop receive-only coil for 3 T. T1-weighted, T2-weighted, and time-of-flight bright-blood imaging protocols with comparable settings at 3 T and 7 T resulted in significantly improved vessel-wall SNR and lumen-wall CNR for 7 T. Comparable accuracy was achieved for luminal and vessel wall areas.

Koning et al[27] introduced a different coil design for 7 T carotid MRI consisting of separate transmit and receive array coils. The advantage of separating transmission from reception is that both can be individually tailored for optimal performance. The receiver coil consisted of a 2×15-channel array for both sides of the neck, which can be placed near the carotid arteries for optimal sensitivity and parallel imaging performance. The 2-channel transmission coil comprised radiative antennas and were placed more distant from the neck on a flexible neck pillow filled with deuterium-oxide as a dielectric

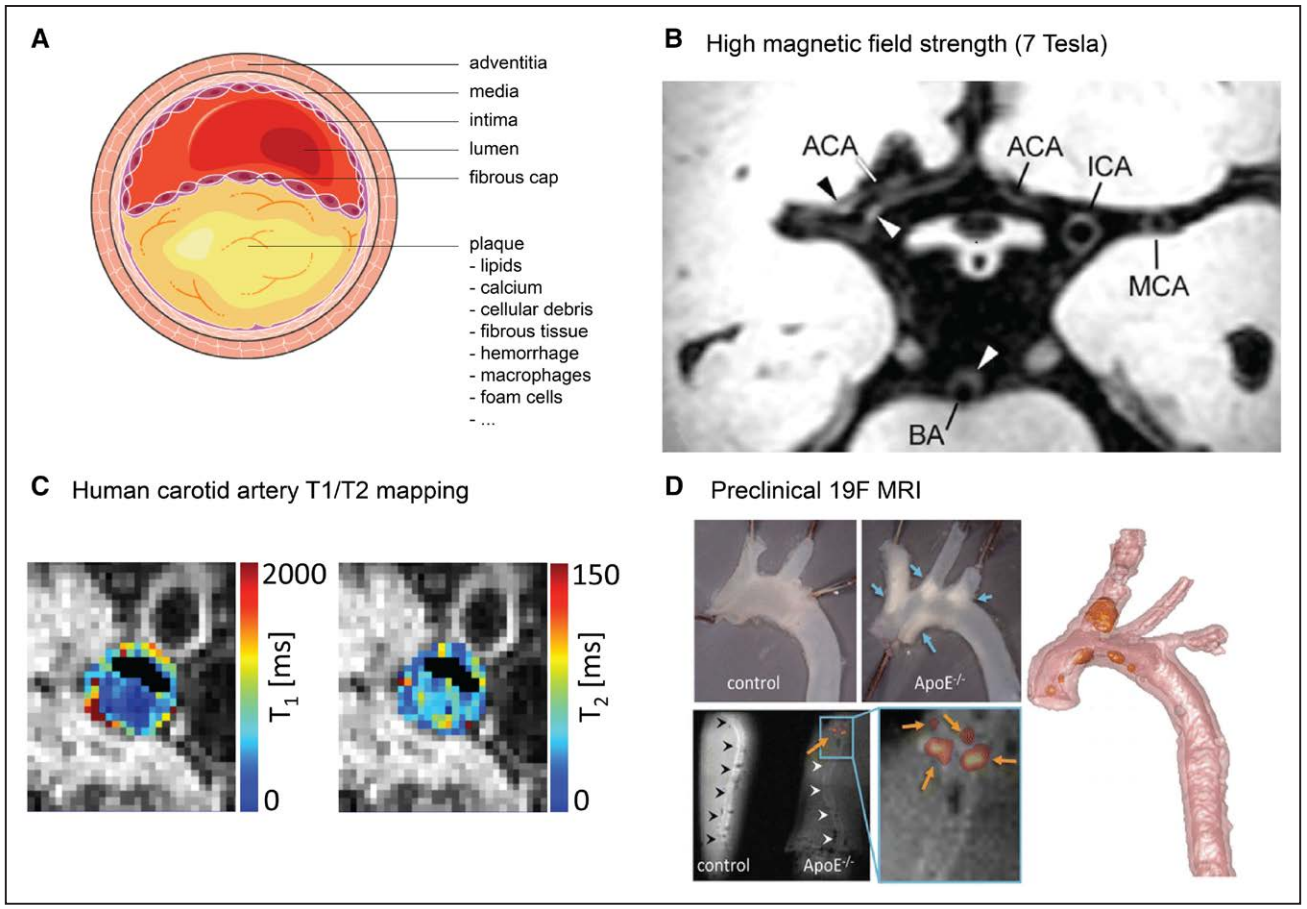

Figure. Emerging magnetic resonance imaging (MRI) techniques for atherosclerosis imaging. **A**, Schematic of an atherosclerotic plaque in an artery wall. **B**, High-field (7 T) MRI of intracranial vessels in a symptomatic patient. Arrowheads indicate locations of focal thickening of the vessel wall. Adapted from Harteveld et al[38] with permission. Copyright ©2019, Wolters Kluwer Health, Inc. **C**, Axial slice from a 3D quantitative T1 and T2 mapping acquisition of the carotid of a patient with a large atherosclerotic plaque and significant stenosis. Plaque and vessel wall T1 and T2 values are color coded according to the scales next to the images. Lower T1 and slightly elevated T2 values in the plaque are indicative for intraplaque hemorrhage. **D**, Preclinical ^{19}F-MRI of the aortic arch of a control mouse and an atherosclerotic ApoE$^{-/-}$ mouse. **Top**, Ex vivo photographs of the excised aortas. Arrows indicate plaque locations. **Bottom**, Ex vivo ^{19}F-MRI of the aortas. The ^{19}F signal intensity is overlaid in orange/red colors on the regular ^{1}H-MRI. Arrows indicate ^{19}F signals in the plaques. **Right**, 3D rendering of the mouse aorta with ^{19}F signal. Adapted from van Heeswijk et al[65] with permission. Copyright ©2018, Radiological Society of North America. ACA indicates anterior cerebral artery; BA, basilar artery; ICA, intracranial internal carotid artery; and MCA, middle cerebral artery.

substrate. The design offered reasonable transmit homogeneity while preventing high local energy deposition specific absorption rate associated with small transmission coils placed directly on the skin. The performance of this coil was evaluated in comparison to 3 T imaging in healthy subjects and patients with carotid stenosis.[28] An average 2-fold gain in SNR was achieved at 7 T compared with 3 T. The coil was also tested in a cohort of patients with symptomatic stenosis (>70%) of the internal carotid artery, scheduled for endarterectomy.[29] The 7 T MRI scans enabled adequate determinations of vessel lumen and vessel wall areas. However, essentially no correlations were found between vessel wall contrast and histological findings of the excised plaque, apart from absence of signal with calcifications. This shows that merely the gain in SNR associated with the use of 7 T does not guarantee improved plaque composition characterization.

High resolution and good definition of the vessel wall and plaque are essential for accurate plaque size and composition assessment. Currently, a voxel size of 0.4×0.4×2 mm by 3D carotid artery black-blood T2-weighted imaging was demonstrated by Calcagno et al[30] using a 2×4-element transmit/receive array. Adequate suppression of the bright signal from blood in the vessel lumen is required to prevent bleeding of blood signal into the artery wall and partial volume contamination. However, the use of local transmission coils limits efficient inflowing blood suppression, particularly in the carotid arteries where blood flow is high. To tackle this problem, Papoutsis et al recently introduced a carotid artery imaging coil consisting of a 2×2-channel transmission array combined with a 2×2-channel receiver.[31] The receiver coils and 2 transmission elements were placed at the level of the carotid bifurcation. The other 2 transmission elements were placed at the lower part of the neck. The extended coverage of the radiofrequency transmission coils ensured efficient black-blood imaging with good wall/lumen definition using DANTE (delay alternating with nutation for tailored excitation) preparation pulses for blood signal suppression. Although 7 T has demonstrated potential for improved 3D high-resolution vessel wall imaging, resolving certain anatomic details, such as the thin fibrous cap in vulnerable plaques, may still be beyond the capabilities of the current technology. Furthermore, pulsatile motion artifacts which become apparent at the higher 7 T image resolutions

will require further optimization, while preserving reasonable imaging times. For example, although current high-resolution 3D sequences are typically used without the use of cardiac gating, this may become beneficial beyond a certain spatial resolution (eg, <0.5 mm).

MRI of Intracranial Vessels

Similar to carotid atherosclerosis, disorders of the vasculature in the brain pose a significant risk to physical and cognitive health. Because of their smaller sizes, imaging of the intracranial vessel wall may especially benefit from improved resolution facilitated by the higher SNR associated with 7 T.[32] Since the advent of 7 T MRI scanners, imaging of the brain has been a principal application and multiple vendor- and third-party coil designs for optimized radiofrequency transmission and receive sensitivity are readily available for intracranial angiography and vessel wall imaging.[33]

A particular requirement for accurate intracranial vessel wall imaging is that both the signal from the blood and the CSF lining the arteries needs to be suppressed. Blood suppression strategies that have been applied to the carotid arteries may also be applied to suppress the blood signal in the brain. These include double-inversion recovery[34] as well as motion sensitized prepulses such as MSDE (motion sensitized driven equilibrium)[35] and DANTE.[36] Problems may occur in regions with slow flow, for example, near the vessel wall and in aneurysms, where motion sensitization becomes ineffective, leading to incomplete blood suppression and overestimation of the vessel wall thickness. Suppression of CSF is even more challenging since CSF flow is slow and the long T1 of CSF, particularly at 7 T, renders inversion-recovery methods to null the signal very time-inefficient.

Despite these technical challenges, several groups have successfully pioneered intracranial vessel wall imaging at 7 T (Figure 1B) in healthy subjects and patients with different vascular conditions.[18,36–42] For example, Harteveld et al[41] studied the presence and location of intracranial vessel wall lesions in patients with recent posterior cerebral circulation ischemia compared with nonsymptomatic controls, using intracranial vessel wall MRI at 7 T. Although no large differences in lesion burden between both groups were observed, this study nevertheless showed that the technical challenges involved with 7 T MRI can be overcome to provide detailed characterization of the intracranial vessel status. Although not primarily focused on imaging the intracranial vessels, a recent study by Obusez et al[18] included more than 100 patients with a range of neurological pathologies and showed that 7 T provided increased conspicuity for brain lesions and revealed new lesions not seen on 1.5 T and 3 T. Certainly, high-field MRI of vessel walls has the potential to alter diagnosis and treatment in the (near) future.

Relaxation Time Mapping

Plaque Component Characterization

MR contrast between different tissues is mainly caused by their different PD or relaxation time constants (T1 for the longitudinal relaxation and T2 for the transverse relaxation). Developed already in the late 90s,[43,44] 2D multicontrast MRI protocols consisting of T1-, T2-, PD-weighted black-blood imaging and time-of-flight angiography are still the standard (pre)clinical research tool for plaque characterization. However, even after 3 decades, these protocols are not part of routine clinical decision-making in patients with suspected vulnerable plaques. This may partly be explained by the fact that plaque component characterization based on these acquisitions has been mostly qualitative by nature, where the presence of specific plaque components has been determined by visual inspection of the relative signal intensities between the plaque and surrounding (muscle) tissue. This approach can easily lead to large intraobserver variability as well as inconsistent clinical conclusions, depending on the choice of sequence parameters.[45,46] In the last decades, however, many new acquisitions and analysis pipelines have been developed with the potential for a quantitative and user-independent plaque component classification, as described further in this section.

A promising new development toward robust plaque phenotyping is the recent introduction of quantitative parameter mapping techniques, aimed at quantifying plaque T1 and T2 relaxation times, which may more directly reflect plaque composition (Figure 1C). Quantitative relaxation mapping has already started to replace qualitative imaging sequences in cardiac imaging, which has facilitated the standardization of protocols and threshold values to help clinicians diagnose cardiac pathologies.[47] Although an easy translation of such methods to atherosclerosis imaging has been complicated by the need for robust blood suppression, recent studies have applied, with success, these quantitative methods to vessel wall imaging, especially in the carotid arteries.

The first robust quantitative vessel wall MRI protocol was presented by Biasiolli et al,[48] in which T2 quantification of carotid plaques was achieved by a 2D cardiac gated multi-echo spin echo sequence, preceded by a double-inversion blood suppression preparation. This method provided solid T2 reference values for different plaque components, such as lipid-rich necrotic core (T2=37±5 ms), fibrous tissue (T2=56±9 ms), and intraplaque hemorrhage (T2 >90 ms). Moreover, the technique of T2 mapping to estimate the lipid area within plaques discriminated symptomatic and asymptomatic patients,[49] as well as detected a reduction of lipid content within the plaque after 3 months of statin treatment.[50]

The addition of T1 mapping may further improve identification of important biomarkers of plaque vulnerability, such as a fresh intraplaque hemorrhage.[48] Two protocols for T1 mapping have recently been introduced, either based on variable flip angle steady-state[51] or inversion-recovery prepared imaging sequences.[52,53] These protocols were designed for combined T1 and T2 estimation and can be applied at 3D isotropic (0.7–0.8 mm) resolution. While Coolen et al[51] mainly focused on achieving efficient blood suppression for all individual images used for T1 and T2 quantification, this was not possible for the method recently proposed by Qi et al[53] On the contrary, the latter method used efficient 3D radial k-space trajectories making imaging times significantly shorter. Unfortunately, T1 mapping has not been applied so far in large patient groups to assess its predictive value for plaque vulnerability.

The accuracy of quantitative T1 and T2 values increases when more data points (ie, with more inversion or echo times) are acquired. This may require protocols that exceed clinically feasible imaging times. In this respect, the introduction of advanced iterative reconstruction algorithms, such as compressed sensing and machine learning allows for reductions in the amount of data (and hence scanning time) necessary for image reconstruction, and are now increasingly used in clinical quantitative vessel wall imaging.[54–56]

Quantifying Contrast Agent Dynamics

The use of untargeted contrast agents in MR atherosclerosis imaging can be categorized into roughly 2 approaches. The first is aimed at measuring plaque inflammation using T2* shortening by iron oxide particles and, the second approach aims to visualize plaque permeability by dynamic contrast-enhanced MRI using untargeted gadolinium-based MR contrast agents. For both applications, the need for quantitative readouts is eminent.

Iron oxide nanoparticulate contrast agents are taken up by phagocytic cells, and their cellular accumulation can be detected as signal loss by T2$^{(*)}$-weighted MRI. The ATHEROMA trial (Atorvastatin Therapy: Effects on Reduction of Macrophage Activity)[15] was the first prospective MRI study to show the effects of statin therapy on carotid plaque inflammation using iron oxide contrast agents in combination with T2*-weighted imaging. However, it was also criticized because of the qualitative nature of the methodology.[57] This has inspired other researchers to develop quantitative T2* mapping using 2D[58,59] or 3D[54,55] black-blood multigradient-echo sequences to improve scan-rescan reproducibility by the use of $\Delta R2^* (=1/T2^*_{post} - 1/T2^*_{pre})$ as a semiquantitative measure of iron particle accumulation. For these protocols, the earlier mentioned compressed sensing techniques have yet to be applied.

Although considerable success has been achieved with iron oxide contrast agents, it remains nontrivial to detect and particularly quantify inflammation from the iron oxide–induced signal voids. Furthermore, once present in the plaque, the iron oxide–induced contrast changes hamper the quantification of plaque composition by traditional multicontrast MRI (eg, T1 and T2) and dynamic contrast-enhanced imaging with gadolinium contrast to evaluate plaque permeability.

The quantification of plaque permeability using analysis of signal intensity time curves after contrast agent injection comes with many limitations,[19] mostly related to incorrect assumptions of signal linearity of the arterial input function and because of the assumption of a single precontrast T1 despite obvious field inhomogeneity in the plaque. Recently, Wang et al[60] have presented groundbreaking work to overcome these limitations by the introduction of a quantitative T1 mapping dynamic contrast-enhanced sequence with a temporal resolution as low as 500 ms. Key to achieving this unprecedented speed is a sophisticated reconstruction method that involves a single reconstruction of the complete 5-dimensional data matrix (3 spatial dimensions, saturation recovery, and dynamic scans) and exploiting the low-rank nature of this acquisition matrix.[61] This protocol allows T1 mapping with high spatiotemporal resolution, providing the necessary data to correctly model the AIF (arterial input function) and plaque response curves for dynamic contrast-enhanced analysis.

Fluorine-19 Imaging

Imaging of Vascular Inflammation

Macrophages play a key role in plaque rupture and thrombogenicity. As such, macrophage density is considered an important contributor to plaque development and subsequent vulnerability to rupture.[62] Plaque uptake of the positron emission tomography tracer ^{18}F fluorodeoxyglucose has been widely used as a noninvasive and sensitive surrogate marker of macrophage density and inflammation in atherosclerosis.[63,64] However, imaging of fluorodeoxyglucose of vascular origin is challenging in tissues with high background metabolic activity, such as in the heart and the brain. Also, the short half-life time of ^{18}F (≈110 min) prevents monitoring of macrophage migration and activity over longer periods of time.

^{19}F-MRI

A promising alternative strategy towards the realization of clinically feasible inflammation and atherosclerosis imaging is the use of fluorinated nanoparticles.[65,66] Fluorinated nanoparticles contain the stable fluorine isotope ^{19}F, which has a spin ½ and a gyromagnetic ratio of 40.08 MHz/T, resulting in 83% the sensitivity of 1H.[67] The human body contains negligible amounts of ^{19}F, which implies that any detected ^{19}F-MRI signal originates from the nanoparticles with little to no background, clearly benefiting quantification purposes. Moreover, unlike the radioactive ^{18}F isotope used in fluorodeoxyglucose-positron emission tomography, the ^{19}F signal does not decay, which enables detection and tracking of the label over extended periods of time. Similar to iron oxides, fluorinated nanoparticles can be tailored by changing size or surface composition to stimulate phagocytosis by inflammatory cells, with the advantage that their accumulation is directly proportional to the ^{19}F-MRI signal and does not interfere with ^{1}H image contrast. This means that fluorinated nanoparticles can be used in combination with regular T1- and T2-weighted ^{1}H MRI, and other contrasts.

The general working hypothesis of imaging of atherosclerosis by ^{19}F-MRI involves phagocytosis of the nanoemulsions by circulating monocytes and macrophages on intravenous injection. The ^{19}F-filled monocytes and macrophages subsequently traffic to the sites of inflammation, where they can be imaged by ^{19}F-MRI once present in sufficiently high concentrations. The ^{19}F signal also accumulates in the body's repositories of immune cells, such as in the liver (Kupffer cells), the lymph nodes, and in the bone marrow.[65] Clearance is via the lungs and the liver.

In the context of inflammation imaging, most ^{19}F-MRI has been performed using nanoemulsions filled with perfluorocarbons. The liquid hydrophobic perfluorocarbon core in these nanoemulsions is surrounded by a lipid monolayer in which additional targeting ligands (or even gadolinium-contrast agents) can be incorporated.[66,68] Different perfluorocarbons are available, including perfluorodichlorooctane, perfluorodecalin, perfluoro 15-crown-5 ether, and perfluorooctyl bromide. Typically these nanoemulsions have a clearance half-life time

of 3 to 6 hours, depending on size (typically 100–400 nm) and species.[69] This imaging technique has great potential and has been explored, so far, in a variety of preclinical studies on Alzheimer disease,[70] lung imaging,[71] cancer,[72,73] (re)stenosis,[74] cell tracking,[75,76] myocardial infarction and stroke,[77,78] and inflammatory bowel disease.[79]

Fluorine Imaging and Atherosclerosis

The first use of perfluorocarbon nanoparticles for detecting ex vivo atherosclerotic plaques was reported in 2004.[80] A first convincing in vivo demonstration of plaque inflammation imaging by ^{19}F-MRI, albeit not in humans but in a mouse model, is only as recent as 2015.[65] A perfluorocarbon-containing nanoemulsion was injected in ApoE$^{-/-}$ mice, a well-known mouse model of atherosclerosis, and imaged up to 14 days after injection. The ^{19}F signal was observed in the aortic arch, the carotid arteries, and the brachiocephalic artery, known regions where atherosclerotic plaques develop in this mouse model (Figure 1D). Ex vivo 3D visualization of segmented high spatial resolution 3D MRI of the atherosclerotic plaques in the excised aortic arches and their branching vessels confirmed that the source of the ^{19}F was indeed from within the atherosclerotic vessel wall. Importantly, immune-fluorescent staining for macrophages and perfluorocarbon demonstrated the colocalization of both fluorescent signals, confirming that the ^{19}F signal particularly originated from the macrophages located within the atherosclerotic plaques. However, cells that were not macrophages also absorbed perfluorocarbon, suggestive that other cell types are also capable of phagocytosis of these perfluorocarbon nanoparticles. Future work will be necessary to study the specificity of ^{19}F phagocytosis by immune cells and whether these can be of prognostic value.

Depending on their size, perfluorocarbon nanoemulsions may also passively diffuse into the intimal space of the plaque or inflammatory cells located there. In the early stages of atherosclerosis, the proinflammatory status of the vasculature causes the endothelial layer to be weakened or leaky, resulting in a higher permeability of macromolecules through the endothelial barrier. Zhang et al[81] investigated this phenomenon in rabbits fed with a high-fat diet for up to 14 months. Twelve hours after injection of emulsions with varying nominal diameter, ex vivo ^{19}F-MRI scans revealed the features of endothelial barrier disruption and rapid penetration of nanoparticles, even up to micron size, was observed far into the intima of later-stage, but not early-stage, plaques. Thus, apart from active transport of perfluorocarbon emulsions into the plaque by macrophages, also passive accumulation might attribute to the ^{19}F-signal in the plaques. It therefore remains to be further investigated how specific and quantitative vascular inflammation imaging by ^{19}F-MRI technology is.

Technical Considerations

Although the intrinsic ^{19}F-MRI detection sensitivity is close to the one of ^{1}H and there is essentially no native ^{19}F in the human body, it remains challenging to detect and quantify the ^{19}F signal from low concentrations of nanoparticles. The actual detection sensitivity depends on many experimental factors, including the total acquisition time, number of averages, sequence type, image resolution, etc The detection sensitivity in mice is typically in the low millimolar range using sequences and hardware optimized for small animal imaging,[82] resulting in reasonable acquisition times (≈10 min). Most ^{19}F perfluorocarbon resonances have relatively long T1 and T2 relaxation times,[82] which favors 3D imaging with balanced SSFP and turbo-spin-echo sequences.[83] In the case of perfluorocarbons, these relaxation times may also depend on temperature,[82,84] magnetic field strength,[84] and tissue oxygenation level.[85] The introduction of new ^{19}F compounds requires reassessment of the relaxation time properties and optimization of sequence parameters.

There are several exciting new developments in ^{19}F-MRI that make the technique even more attractive. Since the ^{19}F-agent accumulates at sites of active inflammation, the ^{19}F-signal will often be localized rather than dispersed. This can be exploited in modern image acquisition and reconstruction strategies such as compressed sensing[86,87] to maximize the signal-to-noise per unit time or reduce acquisition times to clinically acceptable numbers. Moreover, different fluorinated compounds can be detected on the basis of differences in chemical shift and imaged independently from each other (ie, multiplexed) in the same imaging session, offering unique opportunities to image different populations of inflammatory cells in the same subject.[88,89] One major concern for the translation of ^{19}F-MRI into daily clinical practice is the long half-life time of the particles, which can be up to several months for certain types of nanoemulsions.[90]

Summary and Future Outlook

In this article, we reviewed some of the important emerging MRI techniques for improved atherosclerosis imaging, namely (1) high spatial resolution, high signal-to-noise imaging at clinical 7 T, (2) quantitative T1/T2(*) mapping for improved plaque characterization, and (3) quantitative ^{19}F inflammation imaging.

Technical challenges with field and transmit inhomogeneities, as well as patient discomfort, are currently still impeding the use of field strengths beyond 7 T.[91] However, the general need for higher spatiotemporal resolution in vascular MRI may encourage the use of these higher field strengths. New techniques will have to be developed or optimized to deal with new prominent imaging artifacts emerging at higher spatial resolution, such as pulsatile vessel motion. Acquisitions insensitive to (pulsatile) motion and sophisticated gating techniques—developed to deal with cardiac motion when imaging the coronaries[92]—might also prove beneficial for carotid and intracranial artery imaging.

Protocols for quantitative relaxation time mapping of atherosclerotic plaques in the carotid arteries are ready for clinical use but need more extensive evaluation in large cohort and multicenter studies to establish their added value in comparison to standard techniques. Finally, although the use of ^{19}F MRI for plaque imaging is still in its infancy and currently limited to preclinical applications, it has several advantages (quantitative, no background, and multiplexing) that makes it a promising tool for in vivo plaque phenotyping.

While major advances in MRI of atherosclerosis have been made in the past few decades that have considerably improved

the quantification of plaque burden and characterization of vulnerable plaques, most of these techniques have yet to be translated into (routine) clinical practice. Successful clinical introduction, however, relies on many factors. First of all, the new techniques and hardware (radiofrequency coils) need to become available across the different clinical scanner platforms and optimized for scan time and ease-of-use. Protocols need to be validated for reproducibility. On-line postprocessing of raw image data has to be standardized and integrated in the workflow of data acquisition, (PACS [picture archiving and communication system]) storage, analysis, and viewing. Most importantly, more large-scale clinical research studies across ethnicity, sex, and age are needed to unequivocally demonstrate the added value of these techniques in the management of atherosclerotic disease.

In conclusion, the demand for personalized approaches in the era of precision medicine drives the need for noninvasive diagnostics to identify and characterize at-risk plaque phenotypes noninvasively and in vivo. This will continue to stimulate research into more powerful atherosclerotic MRI protocols and present new opportunities for improved diagnosis and treatment of atherosclerosis.

Sources of Funding

R.C.I. Wüst, M.R.R. Daal, and G.J. Strijkers are supported by a grant from the Dutch Technology Foundation TTW (Toegepaste en Technische Wetenschappen; MUSICIAN [Fluorine Magnetic Resonance and Ultrasound Imaging of Cardiac Inflammation] No. 14716). C. Calcagno is supported by American Heart Association Scientist Development Grant 16SDG27250090. B.F. Coolen is funded by a VENI Grant (No. 14348) from the Dutch Technology Foundation TTW.

Disclosures

None.

References

1. Benjamin EJ, Blaha MJ, Chiuve SE, et al. American Heart Association Statistics Committee and Stroke Statistics Subcommittee. Heart Disease and Stroke Statistics-2017 Update: A Report From the American Heart Association. *Circulation.* 2017;135:e146–e603. doi: 10.1161/CIR.0000000000000485
2. Kolodgie FD, Yahagi K, Mori H, Romero ME, Trout HH Rd, Finn AV, Virmani R. High-risk carotid plaque: lessons learned from histopathology. *Semin Vasc Surg.* 2017;30:31–43. doi: 10.1053/j.semvascsurg.2017.04.008
3. Kerwin WS, Miller Z, Yuan C. Imaging of the high-risk carotid plaque: magnetic resonance imaging. *Semin Vasc Surg.* 2017;30:54–61. doi: 10.1053/j.semvascsurg.2017.04.009
4. Gupta A, Baradaran H, Schweitzer AD, Kamel H, Pandya A, Delgado D, Dunning A, Mushlin AI, Sanelli PC. Carotid plaque MRI and stroke risk: a systematic review and meta-analysis. *Stroke.* 2013;44:3071–3077. doi: 10.1161/STROKEAHA.113.002551
5. Saam T, Hetterich H, Hoffmann V, Yuan C, Dichgans M, Poppert H, Koeppel T, Hoffmann U, Reiser MF, Bamberg F. Meta-analysis and systematic review of the predictive value of carotid plaque hemorrhage on cerebrovascular events by magnetic resonance imaging. *J Am Coll Cardiol.* 2013;62:1081–1091. doi: 10.1016/j.jacc.2013.06.015
6. McDermott MM, Kramer CM, Tian L, et al. Plaque Composition in the Proximal Superficial Femoral Artery and Peripheral Artery Disease Events. *JACC Cardiovasc Imaging.* 2017;10:1003–1012. doi: 10.1016/j.jcmg.2016.08.012
7. Papini GD, Di Leo G, Bandirali M, Cotticelli B, Flor N, Restivo P, Nano G, Sardanelli F. Is Carotid Plaque Contrast Enhancement on MRI Predictive for Cerebral or Cardiovascular Events? A Prospective Cohort Study. *J Comput Assist Tomogr.* 2017;41:321–326. doi: 10.1097/RCT.0000000000000506
8. Xu D, Hippe DS, Underhill HR, Oikawa-Wakayama M, Dong L, Yamada K, Yuan C, Hatsukami TS. Prediction of high-risk plaque development and plaque progression with the carotid atherosclerosis score. *JACC Cardiovasc Imaging.* 2014;7:366–373. doi: 10.1016/j.jcmg.2013.09.022
9. Mani V, Muntner P, Gidding SS, Aguiar SH, El Aidi H, Weinshelbaum KB, Taniguchi H, van der Geest R, Reiber JH, Bansilal S, Farkouh M, Fuster V, Postley JE, Woodward M, Fayad ZA. Cardiovascular magnetic resonance parameters of atherosclerotic plaque burden improve discrimination of prior major adverse cardiovascular events. *J Cardiovasc Magn Reson.* 2009;11:10. doi: 10.1186/1532-429X-11-10
10. Lobatto ME, Calcagno C, Metselaar JM, Storm G, Stroes ES, Fayad ZA, Mulder WJ. Imaging the efficacy of anti-inflammatory liposomes in a rabbit model of atherosclerosis by non-invasive imaging. *Methods Enzymol.* 2012;508:211–228. doi: 10.1016/B978-0-12-391860-4.00011-2
11. Lobatto ME, Calcagno C, Otten MJ, Millon A, Ramachandran S, Paridaans MP, van der Valk FM, Storm G, Stroes ES, Fayad ZA, Mulder WJ, Metselaar JM. Pharmaceutical development and preclinical evaluation of a GMP-grade anti-inflammatory nanotherapy. *Nanomedicine.* 2015;11:1133–1140. doi: 10.1016/j.nano.2015.02.020
12. Vucic E, Calcagno C, Dickson SD, et al. Regression of inflammation in atherosclerosis by the LXR agonist R211945: a noninvasive assessment and comparison with atorvastatin. *JACC Cardiovasc Imaging.* 2012;5:819–828. doi: 10.1016/j.jcmg.2011.11.025
13. Vucic E, Dickson SD, Calcagno C, Rudd JH, Moshier E, Hayashi K, Mounessa JS, Roytman M, Moon MJ, Lin J, Tsimikas S, Fisher EA, Nicolay K, Fuster V, Fayad ZA. Pioglitazone modulates vascular inflammation in atherosclerotic rabbits noninvasive assessment with FDG-PET-CT and dynamic contrast-enhanced MR imaging. *JACC Cardiovasc Imaging.* 2011;4:1100–1109. doi: 10.1016/j.jcmg.2011.04.020
14. Fayad ZA, Mani V, Woodward M, Kallend D, Abt M, Burgess T, Fuster V, Ballantyne CM, Stein EA, Tardif JC, Rudd JH, Farkouh ME, Tawakol A; dal-PLAQUE Investigators. Safety and efficacy of dalcetrapib on atherosclerotic disease using novel non-invasive multimodality imaging (dal-PLAQUE): a randomised clinical trial. *Lancet.* 2011;378:1547–1559. doi: 10.1016/S0140-6736(11)61383-4
15. Tang TY, Howarth SP, Miller SR, et al. The ATHEROMA (Atorvastatin Therapy: Effects on Reduction of Macrophage Activity) Study. Evaluation using ultrasmall superparamagnetic iron oxide-enhanced magnetic resonance imaging in carotid disease. *J Am Coll Cardiol.* 2009;53:2039–2050. doi: 10.1016/j.jacc.2009.03.018
16. Balu N, Yarnykh VL, Chu B, Wang J, Hatsukami T, Yuan C. Carotid plaque assessment using fast 3D isotropic resolution black-blood MRI. *Magn Reson Med.* 2011;65:627–637. doi: 10.1002/mrm.22642
17. Fan Z, Zhang Z, Chung YC, Weale P, Zuehlsdorff S, Carr J, Li D. Carotid arterial wall MRI at 3T using 3D variable-flip-angle turbo spin-echo (TSE) with flow-sensitive dephasing (FSD). *J Magn Reson Imaging.* 2010;31:645–654. doi: 10.1002/jmri.22058
18. Obusez EC, Lowe M, Oh SH, et al. 7T MR of intracranial pathology: Preliminary observations and comparisons to 3T and 1.5T. *Neuroimage.* 2018;168:459–476. doi: 10.1016/j.neuroimage.2016.11.030
19. Coolen BF, Calcagno C, van Ooij P, Fayad ZA, Strijkers GJ, Nederveen AJ. Vessel wall characterization using quantitative MRI: what's in a number? *MAGMA.* 2018;31:201–222. doi: 10.1007/s10334-017-0644-x
20. Runge VM. Critical Questions Regarding Gadolinium Deposition in the Brain and Body After Injections of the Gadolinium-Based Contrast Agents, Safety, and Clinical Recommendations in Consideration of the EMA's Pharmacovigilance and Risk Assessment Committee Recommendation for Suspension of the Marketing Authorizations for 4 Linear Agents. *Invest Radiol.* 2017;52:317–323. doi: 10.1097/RLI.0000000000000374
21. Vasanawala SS, Nguyen KL, Hope MD, Bridges MD, Hope TA, Reeder SB, Bashir MR. Safety and technique of ferumoxytol administration for MRI. *Magn Reson Med.* 2016;75:2107–2111. doi: 10.1002/mrm.26151
22. Kraff O, Bitz AK, Orzada S, Maderwald S, Kruszona S, Schaefer LC, Grootfaam JY, Ladd ME, Quick HH. An Eight-Channel Transmit/Receive RF Array for Imaging the Carotid Arteries at 7 Tesla. *Proc. Intl. Soc. Mag. Reson. Med.* 2009;17:3007
23. Wiggins G, Zhang B, Duan Q, Lattanzi R, Biber S, Stoeckel B, McGorty K, Sodickson DK. 7 Tesla Transmit-Receive Array for Carotid Imaging: Simulation and Experiment. *Proc. Intl. Soc. Mag. Reson. Med.* 2009;17:394
24. Breyer T, Kraff O, Maderwald S, Bitz A, Orzada S, Ladd ME, Gizewski ER, Quick HH. Carotid Plaque Imaging with an Eight-Channel Transmit/Receive RF Array at 7 Tesla: First Results in Patients with Atherosclerosis. *Proc. Intl. Soc. Mag. Reson. Med.* 2010;18:3684
25. Kraff O, Bitz AK, Breyer T, Kruszona S, Maderwald S, Brote I, Gizewski ER, Ladd ME, Quick HH. A transmit/receive radiofrequency array for imaging the carotid arteries at 7 Tesla: coil design and first

in vivo results. *Invest Radiol.* 2011;46:246–254. doi: 10.1097/RLI.0b013e318206cee4
26. Kröner ES, van Schinkel LD, Versluis MJ, Brouwer NJ, van den Boogaard PJ, van der Wall EE, de Roos A, Webb AG, Siebelink HM, Lamb HJ. Ultrahigh-field 7-T magnetic resonance carotid vessel wall imaging: initial experience in comparison with 3-T field strength. *Invest Radiol.* 2012;47:697–704. doi: 10.1097/RLI.0b013e31826dc174
27. Koning W, Bluemink JJ, Langenhuizen EA, Raaijmakers AJ, Andreychenko A, van den Berg CA, Luijten PR, Zwanenburg JJ, Klomp DW. High-resolution MRI of the carotid arteries using a leaky waveguide transmitter and a high-density receive array at 7 T. *Magn Reson Med.* 2013;69:1186–1193. doi: 10.1002/mrm.24345
28. Koning W, de Rotte AA, Bluemink JJ, van der Velden TA, Luijten PR, Klomp DW, Zwanenburg JJ. MRI of the carotid artery at 7 Tesla: quantitative comparison with 3 Tesla. *J Magn Reson Imaging.* 2015;41:773–780. doi: 10.1002/jmri.24601
29. de Rotte AA, Koning W, Truijman MT, den Hartog AG, Bovens SM, Vink A, Sepehrkhouy S, Zwanenburg JJ, Klomp DW, Pasterkamp G, Moll FL, Luijten PR, Hendrikse J, de Borst GJ. Seven-tesla magnetic resonance imaging of atherosclerotic plaque in the significantly stenosed carotid artery: a feasibility study. *Invest Radiol.* 2014;49:749–757. doi: 10.1097/RLI.0000000000000079
30. Calcagno C, Coolen BF, Zhang B, Boeykens G, Robson P, Mani V, Nederveen AJ, Mulder W, Fayad Z. Optimization of 3 dimensional (3D), high resolution T2 weighted SPACE for carotid vessel wall imaging on a 7T whole-body clinical scanner. *Proc. Intl. Soc. Mag. Reson. Med.* 2016;24:0968
31. Papoutsis K, Li L, Near J, Payne S, Jezzard P. A purpose-built neck coil for black-blood DANTE-prepared carotid artery imaging at 7T. *Magn Reson Imaging.* 2017;40:53–61. doi: 10.1016/j.mri.2017.04.011
32. De Cocker LJ, Lindenholz A, Zwanenburg JJ, van der Kolk AG, Zwartbol M, Luijten PR, Hendrikse J. Clinical vascular imaging in the brain at 7T. *Neuroimage.* 2018;168:452–458. doi: 10.1016/j.neuroimage.2016.11.044
33. Kang CK, Woo MK, Hong SM, Kim YB, Cho ZH. Intracranial microvascular imaging at 7 T MRI with transceiver RF coils. *Magn Reson Imaging.* 2014;32:1133–1138. doi: 10.1016/j.mri.2014.07.006
34. Edelman RR, Chien D, Kim D. Fast selective black blood MR imaging. *Radiology.* 1991;181:655–660. doi: 10.1148/radiology.181.3.1947077
35. Wang J, Yarnykh VL, Hatsukami T, Chu B, Balu N, Yuan C. Improved suppression of plaque-mimicking artifacts in black-blood carotid atherosclerosis imaging using a multislice motion-sensitized driven-equilibrium (MSDE) turbo spin-echo (TSE) sequence. *Magn Reson Med.* 2007;58:973–981. doi: 10.1002/mrm.21385
36. Viessmann O, Li L, Benjamin P, Jezzard P. T2-Weighted intracranial vessel wall imaging at 7 Tesla using a DANTE-prepared variable flip angle turbo spin echo readout (DANTE-SPACE). *Magn Reson Med.* 2017;77:655–663. doi: 10.1002/mrm.26152
37. van der Kolk AG, Zwanenburg JJ, Denswil NP, Vink A, Spliet WG, Daemen MJ, Visser F, Klomp DW, Luijten PR, Hendrikse J. Imaging the intracranial atherosclerotic vessel wall using 7T MRI: initial comparison with histopathology. *AJNR Am J Neuroradiol.* 2015;36:694–701. doi: 10.3174/ajnr.A4178
38. Harteveld AA, van der Kolk AG, Zwanenburg JJ, Luijten PR, Hendrikse J. 7-T MRI in Cerebrovascular Diseases: Challenges to Overcome and Initial Results. *Top Magn Reson Imaging.* 2016;25:89–100. doi: 10.1097/RMR.0000000000000080
39. Zhu C, Haraldsson H, Tian B, Meisel K, Ko N, Lawton M, Grinstead J, Ahn S, Laub G, Hess C, Saloner D. High resolution imaging of the intracranial vessel wall at 3 and 7 T using 3D fast spin echo MRI. *MAGMA.* 2016;29:559–570. doi: 10.1007/s10334-016-0531-x
40. Wermer MJ, van Walderveen MA, Garpebring A, van Osch MJ, Versluis MJ. 7Tesla MRA for the differentiation between intracranial aneurysms and infundibula. *Magn Reson Imaging.* 2017;37:16–20. doi: 10.1016/j.mri.2016.11.006
41. Harteveld AA, van der Kolk AG, van der Worp HB, Dieleman N, Zwanenburg JJM, Luijten PR, Hendrikse J. Detecting Intracranial Vessel Wall Lesions With 7T-Magnetic Resonance Imaging: Patients With Posterior Circulation Ischemia Versus Healthy Controls. *Stroke.* 2017;48:2601–2604. doi: 10.1161/STROKEAHA.117.017868
42. Harteveld AA, van der Kolk AG, van der Worp HB, Dieleman N, Siero JC, Kuijf HJ, Frijns CJ, Luijten PR, Zwanenburg JJ, Hendrikse J. High-resolution intracranial vessel wall MRI in an elderly asymptomatic population: comparison of 3T and 7T. *Eur Radiol.* 2017;27:1585–1595. doi: 10.1007/s00330-016-4483-3
43. Fayad ZA, Fuster V. Characterization of atherosclerotic plaques by magnetic resonance imaging. *Ann N Y Acad Sci.* 2000;902:173–186.
44. Yuan C, Mitsumori LM, Beach KW, Maravilla KR. Carotid atherosclerotic plaque: noninvasive MR characterization and identification of vulnerable lesions. *Radiology.* 2001;221:285–299. doi: 10.1148/radiol.2212001612
45. Sun J, Zhao XQ, Balu N, et al. Carotid magnetic resonance imaging for monitoring atherosclerotic plaque progression: a multicenter reproducibility study. *Int J Cardiovasc Imaging.* 2015;31:95–103. doi: 10.1007/s10554-014-0532-7
46. Gao S, van 't Klooster R, van Wijk DF, Nederveen AJ, Lelieveldt BP, van der Geest RJ. Repeatability of *in vivo* quantification of atherosclerotic carotid artery plaque components by supervised multispectral classification. *MAGMA.* 2015;28:535–545. doi: 10.1007/s10334-015-0495-2
47. Messroghli DR, Moon JC, Ferreira VM, Grosse-Wortmann L, He T, Kellman P, Mascherbauer J, Nezafat R, Salerno M, Schelbert EB, Taylor AJ, Thompson R, Ugander M, van Heeswijk RB, Friedrich MG. Clinical recommendations for cardiovascular magnetic resonance mapping of T1, T2, T2* and extracellular volume: A consensus statement by the Society for Cardiovascular Magnetic Resonance (SCMR) endorsed by the European Association for Cardiovascular Imaging (EACVI). *J Cardiovasc Magn Reson.* 2017;19:75. doi: 10.1186/s12968-017-0389-8
48. Biasiolli L, Lindsay AC, Chai JT, Choudhury RP, Robson MD. In-vivo quantitative T2 mapping of carotid arteries in atherosclerotic patients: segmentation and T2 measurement of plaque components. *J Cardiovasc Magn Reson.* 2013;15:69. doi: 10.1186/1532-429X-15-69
49. Chai JT, Biasiolli L, Li L, Alkhalil M, Galassi F, Darby C, Halliday AW, Hands L, Magee T, Perkins J, Sideso E, Handa A, Jezzard P, Robson MD, Choudhury RP. Quantification of Lipid-Rich Core in Carotid Atherosclerosis Using Magnetic Resonance T2 Mapping: Relation to Clinical Presentation. *JACC Cardiovasc Imaging.* 2017;10:747–756. doi: 10.1016/j.jcmg.2016.06.013
50. Alkhalil M, Biasiolli L, Akbar N, Galassi F, Chai JT, Robson MD, Choudhury RP. T2 mapping MRI technique quantifies carotid plaque lipid, and its depletion after statin initiation, following acute myocardial infarction. *Atherosclerosis.* 2018;279:100–106. doi: 10.1016/j.atherosclerosis.2018.08.033
51. Coolen BF, Poot DH, Liem MI, Smits LP, Gao S, Kotek G, Klein S, Nederveen AJ. Three-dimensional quantitative T1 and T2 mapping of the carotid artery: Sequence design and *in vivo* feasibility. *Magn Reson Med.* 2016;75:1008–1017. doi: 10.1002/mrm.25634
52. Qi H, Sun J, Qiao H, Chen S, Zhou Z, Pan X, Wang Y, Zhao X, Li R, Yuan C, Chen H. Carotid Intraplaque Hemorrhage Imaging with Quantitative Vessel Wall T1 Mapping: Technical Development and Initial Experience. *Radiology.* 2018;287:276–284. doi: 10.1148/radiol.2017170526
53. Qi H, Sun J, Qiao H, Zhao X, Guo R, Balu N, Yuan C, Chen H. Simultaneous T1 and T2 mapping of the carotid plaque (SIMPLE) with T2 and inversion recovery prepared 3D radial imaging. *Magn Reson Med.* 2018
54. Yuan J, Graves MJ, Patterson AJ, Priest AN, Ruetten PPR, Usman A, Gillard JH. The development and optimisation of 3D black-blood R2* mapping of the carotid artery wall. *Magn Reson Imaging.* 2017;44:104–110. doi: 10.1016/j.mri.2017.08.006
55. Yuan J, Usman A, Reid SA, King KF, Patterson AJ, Gillard JH, Graves MJ. Three-dimensional black-blood T2 mapping with compressed sensing and data-driven parallel imaging in the carotid artery. *Magn Reson Imaging.* 2017;37:62–69. doi: 10.1016/j.mri.2016.11.014
56. Wu J, Xin J, Sun J, Zhou Z, Chu B, Xu D, Yuan C. An integrative deep learning model to distinguish between normal and atherosclerotic carotid arteries on black-blood vessel wall MRI. *Proc Intl Soc Mag Reson Med.* 2018;26:3484
57. Fayad ZA, Razzouk L, Briley-Saebo KC, Mani V. Iron oxide magnetic resonance imaging for atherosclerosis therapeutic evaluation: still "rusty?". *J Am Coll Cardiol.* 2009;53:2051–2052. doi: 10.1016/j.jacc.2009.03.021
58. Patterson AJ, Tang TY, Graves MJ, Müller KH, Gillard JH. *In vivo* carotid plaque MRI using quantitative T2* measurements with ultrasmall superparamagnetic iron oxide particles: a dose-response study to statin therapy. *NMR Biomed.* 2011;24:89–95. doi: 10.1002/nbm.1560
59. Smits LP, Tiessens F, Zheng KH, Stroes ES, Nederveen AJ, Coolen BF. Evaluation of ultrasmall superparamagnetic iron-oxide (USPIO) enhanced MRI with ferumoxytol to quantify arterial wall inflammation. *Atherosclerosis.* 2017;263:211–218. doi: 10.1016/j.atherosclerosis.2017.06.020
60. Wang N, Christodoulou AG, Xie Y, Wang Z, Deng Z, Zhou B, Lee S, Fan Z, Chang H, Yu W, Li D. Quantitative 3D dynamic contrast-enhanced (DCE) MR imaging of carotid vessel wall by fast T1 mapping using Multitasking. *Magn Reson Med.* 2019;81:2302–2314. doi: 10.1002/mrm.27553

61. Christodoulou AG, Shaw JL, Nguyen C, Yang Q, Xie Y, Wang N, Li D. Magnetic resonance multitasking for motion-resolved quantitative cardiovascular imaging. *Nat Biomed Eng.* 2018;2:215–226. doi: 10.1038/s41551-018-0217-y
62. Swirski FK, Pittet MJ, Kircher MF, Aikawa E, Jaffer FA, Libby P, Weissleder R. Monocyte accumulation in mouse atherogenesis is progressive and proportional to extent of disease. *Proc Natl Acad Sci U S A.* 2006;103:10340–10345. doi: 10.1073/pnas.0604260103
63. Tawakol A, Migrino RQ, Bashian GG, Bedri S, Vermylen D, Cury RC, Yates D, LaMuraglia GM, Furie K, Houser S, Gewirtz H, Muller JE, Brady TJ, Fischman AJ. *In vivo* 18F-fluorodeoxyglucose positron emission tomography imaging provides a noninvasive measure of carotid plaque inflammation in patients. *J Am Coll Cardiol.* 2006;48:1818–1824. doi: 10.1016/j.jacc.2006.05.076
64. Calcagno C, Lairez O, Hawkins J, et al. Combined PET/DCE-MRI in a Rabbit Model of Atherosclerosis: Integrated Quantification of Plaque Inflammation, Permeability, and Burden During Treatment With a Leukotriene A4 Hydrolase Inhibitor. *JACC Cardiovasc Imaging.* 2018;11(2 Pt 2):291–301. doi: 10.1016/j.jcmg.2017.11.030
65. van Heeswijk RB, Pellegrin M, Flögel U, Gonzales C, Aubert JF, Mazzolai L, Schwitter J, Stuber M. Fluorine MR Imaging of Inflammation in Atherosclerotic Plaque in Vivo. *Radiology.* 2015;275:421–429. doi: 10.1148/radiol.14141371
66. Kaneda MM, Caruthers S, Lanza GM, Wickline SA. Perfluorocarbon nanoemulsions for quantitative molecular imaging and targeted therapeutics. *Ann Biomed Eng.* 2009;37:1922–1933. doi: 10.1007/s10439-009-9643-z
67. Reid DG, Murphy PS. Fluorine magnetic resonance in vivo: a powerful tool in the study of drug distribution and metabolism. *Drug Discov Today.* 2008;13:473–480. doi: 10.1016/j.drudis.2007.12.011
68. Southworth R, Kaneda M, Chen J, Zhang L, Zhang H, Yang X, Razavi R, Lanza G, Wickline SA. Renal vascular inflammation induced by Western diet in ApoE-null mice quantified by (19)F NMR of VCAM-1 targeted nanobeacons. *Nanomedicine.* 2009;5:359–367. doi: 10.1016/j.nano.2008.12.002
69. Hu G, Lijowski M, Zhang H, Partlow KC, Caruthers SD, Kiefer G, Gulyas G, Athey P, Scott MJ, Wickline SA, Lanza GM. Imaging of Vx-2 rabbit tumors with alpha(nu)beta3-integrin-targeted 111In nanoparticles. *Int J Cancer.* 2007;120:1951–1957. doi: 10.1002/ijc.22581
70. Tooyama I, Yanagisawa D, Taguchi H, Kato T, Hirao K, Shirai N, Sogabe T, Ibrahim NF, Inubushi T, Morikawa S. Amyloid imaging using fluorine-19 magnetic resonance imaging ((19)F-MRI). *Ageing Res Rev.* 2016;30:85–94. doi: 10.1016/j.arr.2015.12.008
71. Fox MS, Gaudet JM, Foster PJ. Fluorine-19 MRI Contrast Agents for Cell Tracking and Lung Imaging. *Magn Reson Insights.* 2015;8(suppl 1):53–67. doi: 10.4137/MRI.S23559
72. Chapelin F, Capitini CM, Ahrens ET. Fluorine-19 MRI for detection and quantification of immune cell therapy for cancer. *J Immunother Cancer.* 2018;6:105. doi: 10.1186/s40425-018-0416-9
73. Zhang C, Moonshi SS, Wang W, Ta HT, Han Y, Han FY, Peng H, Král P, Rolfe BE, Gooding JJ, Gaus K, Whittaker AK. High F-Content Perfluoropolyether-Based Nanoparticles for Targeted Detection of Breast Cancer by 19F Magnetic Resonance and Optical Imaging. *ACS Nano.* 2018;12:9162–9176. doi: 10.1021/acsnano.8b03726
74. Lanza GM, Yu X, Winter PM, Abendschein DR, Karukstis KK, Scott MJ, Chinen LK, Fuhrhop RW, Scherrer DE, Wickline SA. Targeted antiproliferative drug delivery to vascular smooth muscle cells with a magnetic resonance imaging nanoparticle contrast agent: implications for rational therapy of restenosis. *Circulation.* 2002;106:2842–2847.
75. Bouchlaka MN, Ludwig KD, Gordon JW, Kutz MP, Bednarz BP, Fain SB, Capitini CM. (19)F-MRI for monitoring human NK cells in vivo. *Oncoimmunology.* 2016;5:e1143996. doi: 10.1080/2162402X.2016.1143996
76. Ahrens ET, Flores R, Xu H, Morel PA. *In vivo* imaging platform for tracking immunotherapeutic cells. *Nat Biotechnol.* 2005;23:983–987. doi: 10.1038/nbt1121
77. Flögel U, Ding Z, Hardung H, Jander S, Reichmann G, Jacoby C, Schubert R, Schrader J. *In vivo* monitoring of inflammation after cardiac and cerebral ischemia by fluorine magnetic resonance imaging. *Circulation.* 2008;118:140–148. doi: 10.1161/CIRCULATIONAHA.107.737890
78. van Heeswijk RB, Pilloud Y, Flögel U, Schwitter J, Stuber M. Fluorine-19 magnetic resonance angiography of the mouse. *PLoS One.* 2012;7:e42236. doi: 10.1371/journal.pone.0042236
79. Shin SH, Kadayakkara DK, Bulte JW. *In Vivo* 19F MR Imaging Cell Tracking of Inflammatory Macrophages and Site-specific Development of Colitis-associated Dysplasia. *Radiology.* 2017;282:194–201. doi: 10.1148/radiol.2016152387
80. Morawski AM, Winter PM, Yu X, Fuhrhop RW, Scott MJ, Hockett F, Robertson JD, Gaffney PJ, Lanza GM, Wickline SA. Quantitative "magnetic resonance immunohistochemistry" with ligand-targeted (19)F nanoparticles. *Magn Reson Med.* 2004;52:1255–1262. doi: 10.1002/mrm.20287
81. Zhang H, Zhang L, Myerson J, Bibee K, Scott M, Allen J, Sicard G, Lanza G, Wickline S. Quantifying the evolution of vascular barrier disruption in advanced atherosclerosis with semipermeant nanoparticle contrast agents. *PLoS One.* 2011;6:e26385. doi: 10.1371/journal.pone.0026385
82. Colotti R, Bastiaansen JAM, Wilson A, Flögel U, Gonzales C, Schwitter J, Stuber M, van Heeswijk RB. Characterization of perfluorocarbon relaxation times and their influence on the optimization of fluorine-19 MRI at 3 tesla. *Magn Reson Med.* 2017;77:2263–2271. doi: 10.1002/mrm.26317
83. Flögel U, Ahrens ET. *Fluorine Magnetic Resonance Imaging*. New York: Pan Stanford Publishing; 2016.
84. Kadayakkara DK, Damodaran K, Hitchens TK, Bulte JW, Ahrens ET. (19) F spin-lattice relaxation of perfluoropolyethers: Dependence on temperature and magnetic field strength (7.0-14.1T). *J Magn Reson.* 2014;242:18–22. doi: 10.1016/j.jmr.2014.01.014
85. Duong TQ, Kim SG. *In vivo* MR measurements of regional arterial and venous blood volume fractions in intact rat brain. *Magn Reson Med.* 2000;43:393–402.
86. Kampf T, Fischer A, Basse-Lüsebrink TC, Ladewig G, Breuer F, Stoll G, Jakob PM, Bauer WR. Application of compressed sensing to *in vivo* 3D ^{19}F CSI. *J Magn Reson.* 2010;207:262–273. doi: 10.1016/j.jmr.2010.09.006
87. Kampf T, Sturm VJF, Basse-Lusebrink TC, Fischer A, Buschle LR, Kurz FT, Schlemmer HP, Ziener CH, Heiland S, Bendszus M, Pham M, Stoll G, Jakob PM. Improved compressed sensing reconstruction for 19F magnetic resonance imaging. *Magn Reson Mater Phy*. 2019
88. Akazawa K, Sugihara F, Nakamura T, Matsushita H, Mukai H, Akimoto R, Minoshima M, Mizukami S, Kikuchi K. Perfluorocarbon-Based 19F MRI Nanoprobes for In Vivo Multicolor Imaging. *Angew Chem Int Ed Engl*. 2018
89. van Heeswijk RB, Colotti R, Darçot E, Delacoste J, Pellegrin M, Piccini D, Hernando D. Chemical shift encoding (CSE) for sensitive fluorine-19 MRI of perfluorocarbons with complex spectra. *Magn Reson Med.* 2018;79:2724–2730. doi: 10.1002/mrm.26895
90. Jacoby C, Temme S, Mayenfels F, Benoit N, Krafft MP, Schubert R, Schrader J, Flögel U. Probing different perfluorocarbons for *in vivo* inflammation imaging by 19F MRI: image reconstruction, biological half-lives and sensitivity. *NMR Biomed.* 2014;27:261–271. doi: 10.1002/nbm.3059
91. Ertürk MA, Wu X, Eryaman Y, Van de Moortele PF, Auerbach EJ, Lagore RL, DelaBarre L, Vaughan JT, Uğurbil K, Adriany G, Metzger GJ. Toward imaging the body at 10.5 tesla. *Magn Reson Med.* 2017;77:434–443. doi: 10.1002/mrm.26487
92. Ginami G, Yerly J, Masci PG, Stuber M. Golden angle dual-inversion recovery acquisition coupled with a flexible time-resolved sparse reconstruction facilitates sequence timing in high-resolution coronary vessel wall MRI at 3 T. *Magn Reson Med.* 2017;77:961–969. doi: 10.1002/mrm.26171

Highlights

- There is an unmet need for noninvasive diagnostics to identify and characterize at-risk plaque phenotypes noninvasively and in vivo, to improve the stratification of patients with cardiovascular disease, and for treatment evaluation.
- Physicists are pushing the boundaries of magnetic resonance atherosclerosis imaging to increase image resolution, provide improved quantitative evaluation of plaque constituents, and obtain readouts of disease activity such as inflammation.
- Emerging imaging technologies are high-field magnetic resonance imaging, the use of quantitative relaxation parameter mapping for improved plaque characterization, and novel fluorine-19 magnetic resonance imaging technology to image plaque inflammation.